

## DISORDER OF TETRAHEDRA IN NASICON-TYPE STRUCTURE—I.

### Na<sub>3</sub>Sc<sub>2</sub>(PO<sub>4</sub>)<sub>3</sub>: STRUCTURES AND ION-ION CORRELATIONS

G. COLLIN and R. COMES

Laboratoire de Physique des Solides, U.A. 02 CNRS Bat. 510, Université Paris-Sud,  
91405 Orsay, France

J. P. BOILOT and Ph. COLOMBAN

Groupe de Chimie du Solide, Laboratoire P.M.C. Ecole Polytechnique,  
91128 Palaiseau Cedex, France

(Received 2 October 1985; accepted 13 February 1986)

**Abstract**—The crystal structures of three Nasicon-type Na<sub>3</sub>Sc<sub>2</sub>(PO<sub>4</sub>)<sub>3</sub> single crystals, prepared by different methods, have been examined. The first one ( $\alpha$ ), prepared by fusion, is monoclinic with complete order of Na<sup>+</sup> and vacancies, and strongly displaced positions. The second one ( $\beta$ ), obtained by crystallization of powder at 1470°C, is rhombohedral but with a tri-twinned monoclinic superstructure (2a,c) which corresponds to a long-range ordering distinct from that of the first crystal. The third one ( $\gamma$ ), prepared by flux methods, is also rhombohedral, but with a superstructure (2a,c) of limited coherence length and a Na(1) site appreciably vacant. The final *R* factors were respectively 4.51, 2.35 and 2.34%.

The results establish that the three crystals have the same composition, and a Raman investigation indicates an increasing degree of (PO<sub>4</sub>) disorder with decreasing preparation temperature of crystals. The effect of this static disorder of tetrahedra is to screen the interionic correlations.

**Keywords:** Nasicon structure, X-ray diffraction, superionic conductor, disorder of tetrahedra.

### 1. INTRODUCTION

Nasicon-type materials exhibit very promising properties as superionic conductors and for this reason have been extensively studied in the past few years (see for example the *Proceedings of Solid State Ionics* (1983) in *Solid State Ionics* 9–10). This family of materials is derived from solid solutions (Na□<sub>3</sub>)Zr<sub>2</sub>(PO<sub>4</sub>)<sub>3</sub>–(Na<sub>4</sub>)Zr<sub>2</sub>(SiO<sub>4</sub>)<sub>3</sub>, with a pronounced maximum of conductivity around the composition (Na<sub>3</sub>□)Zr<sub>2</sub>(PSi<sub>2</sub>O<sub>12</sub>) [1].

The basic unit of the Nasicon-type structure is built up from two (ZrO<sub>6</sub>) octahedra separated by three [(P,Si)O<sub>4</sub>] tetrahedra, with which they share corner oxygen ions. These [2(ZrO<sub>6</sub>)–3(M'O<sub>4</sub>)] basic units are packed in a quasi-cubic framework which defines a lattice of intersecting channels where the Na<sup>+</sup> ions are localized. There are essentially two types of Na sites; Na(1) in antiprismatic coordination at the intersection of three conduction channels and Na(2), eight-fold coordinated, within the channels. The lattice symmetry of Nasicon compounds is basically rhombohedral (*R*3c) with a slight monoclinic deformation around the (Na<sub>3</sub>□) composition (*x* = 2).

However, investigations of these materials encounter an apparently insuperable difficulty; up to now it has been impossible to prepare single crystals corresponding to the ideal Nasicon composition. Indeed at the preparation temperature for crystals, even when lowered by the addition of flux, the materials are unstable and exhibit appreciable zirconia losses, es-

pecially around the composition *x* = 2 in the solid solution. This results in a complicated homogeneity range with general formula

$$[\text{Na}_{(1+x+3y)}] [\text{Zr}_{(2-y)} \text{Na}_y] [\text{P}_{(3-x)} \text{Si}_x \text{O}_{12}],$$

with the substitution of a part of the Zr<sup>4+</sup> ions by Na<sup>+</sup> ions [2, 3], and in addition with a large vitreous domain [4, 5]. This is the main reason for the relative lack of interest in these Nasicon materials in spite of their exceptional ionic properties.

However, the properties of Nasicon can be investigated. Indeed the right Na<sup>+</sup>/vacancy ratio for optimum conductivity can be reached spontaneously in “stoichiometric” materials, the so-called Nasicon-analogs with general formula Na<sub>3</sub>M<sub>2</sub><sup>3+</sup>(PO<sub>4</sub>)<sub>3</sub>. Moreover, for these latter materials it is generally possible to prepare single crystals at least suitable for structural investigations. These compounds provide therefore a substitute for ideal Nasicon especially useful for the determination of crystal structures, ionic distributions, ion-ion correlations and conduction mechanisms.

Among the different possible M<sup>3+</sup> cations, scandium Sc<sup>3+</sup>, which exhibits the closest similarity with Zr<sup>4+</sup> (empty *d* levels and essentially identical ionic radius) is especially interesting and was consequently examined very early. However, another problem immediately arises with this material: powders and crystals present conflicting and non-reproducible behavior.

Powders are known to exhibit two first-order phase transitions [6, 7]: (a) from a monoclinic, ionic insulator, low temperature phase to a rhombohedral, ionic conductor, intermediate temperature phase at  $T_1 = 65^\circ\text{C}$  and (b) from this intermediate phase to the high temperature phase, again rhombohedral but with superionic behavior at  $T_2 = 168^\circ\text{C}$ .

In contrast, at the present time published work on crystals do not indicate clearly that they behave in the same way as powders, and there seem to be some marked differences between different crystals. The first problem concerns the low temperature modification for which the available data are somewhat confusing as summarized below.

Efremov and Kalinin [8] concluded after a crystal structure determination that the lattice was monoclinic with  $a = 16.10(1)$  Å,  $b = 9.019(4)$  Å,  $c = 8.928(4)$  Å and  $\gamma = 127.14(4)^\circ$ , space group  $Bb$ . The composition deduced from refinement was  $\text{Na}_{3.00(10)}\text{Sc}_2(\text{PO}_4)_3$  but no details of the refinement procedure were given. However, Kalinin *et al.* [9, 10] reported 40 and  $120^\circ\text{C}$  for the transition temperatures, appreciably different from the values observed for powders.

An earlier contribution came from the discoverer of Nasicon, Hong [11], who examined the crystal structure of another crystal and adopted a rather different monoclinic description  $a = 15.461$  Å,  $b = 9.016$  Å,  $c = 8.913$  Å and  $\gamma = 124.80^\circ$  with the centrosymmetric space group  $B2/b$  and a refined composition  $\text{Na}_{2.30(10)}\text{Sc}_2(\text{PO}_4)_3$ .

Another approach, not directly structural, was provided by Delbecq *et al.* [6] who were especially concerned with the physical properties of polycrystalline samples and reported lattice constants for the monoclinic low temperature phase  $a = 15.407$  Å,  $b = 9.100$  Å,  $c = 8.923$  Å and  $\gamma = 123.60^\circ$ , while Susman *et al.* [12] published for this low temperature phase a set of lattice constants based on the Efremov and Kalinin [8] system:  $a = 16.045(2)$  Å,  $b = 9.066(1)$  Å,  $c = 8.322(2)$  Å and  $\gamma = 126.92(2)^\circ$ .

In contrast, we published structural results [7] showing that at low temperature our single crystals of  $\text{Na}_3\text{Sc}_2(\text{PO}_4)_3$  were not monoclinic but strictly rhombohedral and did not exhibit any first-order phase transition. The composition deduced from refinement was  $\text{Na}_{2.82(3)}\text{Sc}_2(\text{PO}_4)_3$ . These results are in partial agreement with those given by Tran Qui *et al.* [13] who also found a rhombohedral symmetry at room temperature but obtained a rather different composition,  $\text{Na}_{2.52}\text{Sc}_2(\text{PO}_4)_3$ , and noted the occurrence of a long-range ordered superstructure.

In contrast with the confusion over the low temperature phase, available data for the intermediate and high temperature phases agree with rhombohedral symmetry but with different compositions deduced from structural determinations; i.e. 2.64 Na per unit formula at  $T = 200^\circ\text{C}$  [13]; the ideal composition  $\text{Na}_{3.00}$  from Susman *et al.* [12];  $\text{Na}_{2.87(3)}$  at  $100^\circ\text{C}$  and  $\text{Na}_{2.82(3)}$  at  $200^\circ\text{C}$  from Boilot *et al.* [7];

$\text{Na}_{2.80(20)}$  at  $60^\circ\text{C}$  from Lazoryak *et al.* [10]; from 2.85 to 2.97 Na (temperature range  $65\text{--}350^\circ\text{C}$ ) reported by Tchakev *et al.* [14, 15].

We will briefly mention that for the two other  $\text{Na}_3\text{M}_2(\text{PO}_4)_3$  materials, with  $\text{M} = \text{Cr}$  and  $\text{Fe}$ , powders and crystals exhibit at room temperature the same monoclinic deformation and more generally behave in exactly the same way at all temperatures [16–18].

In this paper we will show that the observed differences between  $\text{Na}_3\text{Sc}_2(\text{PO}_4)_3$  single crystals are associated with different preparation conditions, the preparation temperature being the determining parameter. We will also show that there is no “non-stoichiometry” mechanism and that all crystals correspond to the ideal formula. In a subsequent paper we will discuss the thermal behavior of these crystals.

## 2. EXPERIMENTAL

### 2.1. Preparation

The  $\text{Na}_3\text{Sc}_2(\text{PO}_4)_3$  powders were prepared by direct reaction of sodium phosphate and scandium oxide. The single crystals were prepared in three different ways. (a) By a quick fusion of powders. Under these conditions some crystals with pyramid shapes can be extracted but with dimensions which do not exceed 0.5 mm. (b) By direct crystallization from powders by annealing at  $1470^\circ\text{C}$ . The crystals obtained by this method exhibit parallelepiped shapes and are again rather small, with dimensions less than 0.5 mm. (c) By a flux method, with sodium phosphate used as flux, at relatively low temperature  $T = 1100^\circ\text{C}$ . In this way crystals with parallelepiped shapes and with dimensions in the range of millimeters were obtained.

These three preparation methods give crystals which differ somewhat from one another and in particular exhibit different structural characteristics and thermal behavior.

### 2.2. Lattice symmetry, space groups and superstructures

A precise determination of the lattice symmetry was performed at room temperature on a four-cycle diffractometer. The crystals obtained by flux and at  $1470^\circ\text{C}$ , hereafter referred as “flux” and “ $1470^\circ\text{C}$ ” respectively, both exhibit average rhombohedral symmetry, whereas the crystals obtained by fusion, denoted “fusion” crystals, revealed themselves to be clearly monoclinic as indicated in Table 1. Examination of highly exposed diffraction patterns (Fig. 1), obtained from  $\text{MoK}\alpha$  radiations with a bent graphite monochromator, shows that the three crystals exhibit the same reference structure, Nasicon-type  $R\bar{3}c$ , undistorted for the “flux” and “ $1470^\circ\text{C}$ ” crystals and slightly distorted for the “fusion” crystal.

For the “fusion” crystal [Fig. 1(a)], the space group is  $B2/b$  (or  $Bb$ ), which corresponds to the natural subgroup of a distorted  $R\bar{3}c$  lattice, and

Table 1. Trigonal lattice constants of the three different kinds of  $\text{Na}_3\text{Sc}_2(\text{PO}_4)_3$  crystals

Rhombohedral parameters (trigonal description)	Crystal (fusion) <sup>†</sup> $\alpha$ phase	Crystal (1470°C) $\beta$ phase	Crystal (flux) $\gamma$ phase
$a$ (Å)	8.900 (4)	8.928 (1)	8.949 (2)
$b$ (Å)	8.900 (4)	8.927 (1)	8.950 (2)
$c$ (Å)	22.769 (11)	22.276 (3)	22.230 (4)
$\alpha$ (°)	90.70 (3)	90.00 (2)	90.00 (2)
$\beta$ (°)	89.30 (3)	90.01 (2)	89.99 (2)
$\gamma$ (°)	119.86 (2)	119.99 (2)	120.01 (2)

<sup>†</sup> For "fusion" crystal this is one of the three possible indexing schemes, the two others giving similar results. Values in parentheses refer to standard deviations.

keeps the same asymmetric unit as the parent rhombohedron with no additional superstructure spots. The presence of forbidden reflections of  $R\bar{3}C$  ( $h0l$  with  $l = 2n \rightarrow 1$ ) in the reciprocal planes non-orthogonal to  $c_{\text{mono}}^*$  indicates that the structural deformation affects the ionic packing rather substantially.

For the "1470°C" and "flux" crystals, the substructure reflections are sharp and do not exhibit, even at large reciprocal distances for either Weissenberg or four-circle diffractometer data, any indication of separation or of broadening as it would be the case if these crystals were simply tri-twins of the monoclinic modification. This means that they are in a physical state distinct from that of the crystal obtained by fusion. This is confirmed by the fact that both crystals reveal the existence of a superstructure of the trigonal-rhombohedral cell with lattice constants ( $2a, 2a, c$ ) where  $a$  and  $c$  refer to the parent Nasicon lattice parameters given in Table 1. Such a superstructure does not exist for the "fusion" crystal.

For the "1470°C" crystal the superstructure spots are sharp and rather intense [Fig. 1(b)], although much weaker than the regular substructure reflections, while for the "flux" crystal the same spots are weak and diffuse (intensity ratio  $\approx 10^{-1}$ ) with respect to those of the "1470°C" crystal. This indicates a limited coherence length.

To sum up, the examination of these materials immediately shows that we are dealing with three different types of crystals, and this paper will be devoted to the determinations of the physical parameters which lead to this difference.

### 3. THE THREE CRYSTAL TYPES

#### 3.1. The monoclinic modification

3.1.1. *Crystal structure determination.* The lattice constants of the "fusion" crystal are given in the previous section. Data were collected up to  $2\theta = 65^\circ$  ( $\text{MoK}\alpha$ ). After absorption corrections, the whole set of 2007 independent reflections was used in the refinement including the 324 with  $I < 3\sigma$ . This large number of weak reflections is due to the small dimensions of the non-twinned "fusion" crystals with exhibit the correct diffraction spots.

In the first stages the calculations carried out with the usual  $B2/b$  space group of Nasicon [11, 16] led

to a disordered distribution of  $\text{Na}^+$  ions and a rather high  $R$  factor (8.5%)

$$R(\%) = 100 \cdot \Sigma |F_{\text{obs}} - F_{\text{calc}}| / \Sigma F_{\text{obs}}$$

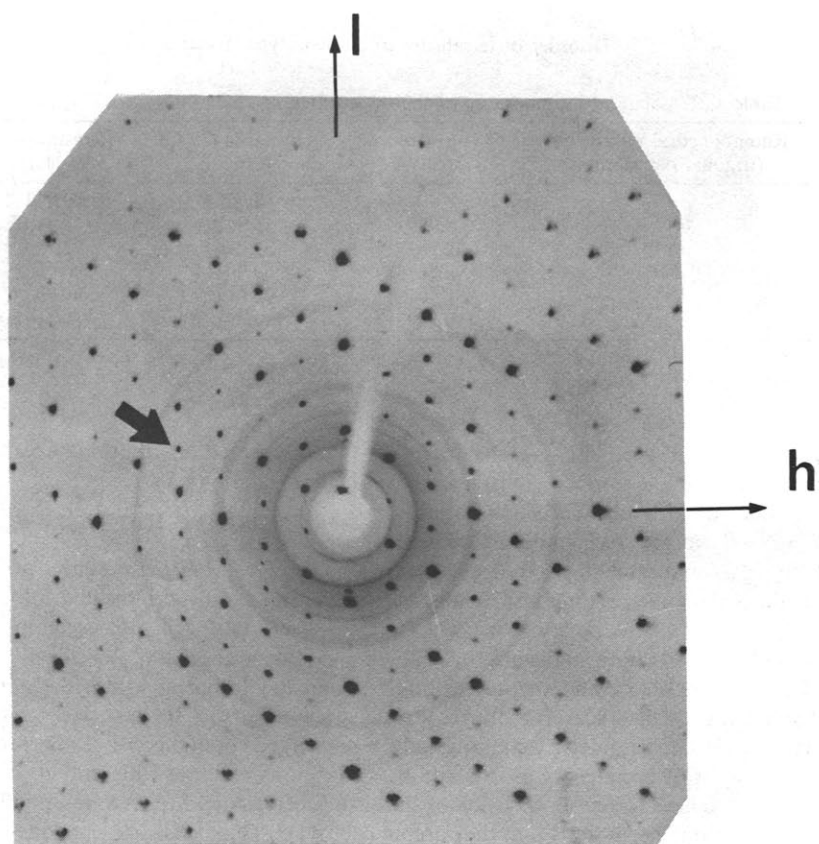
Therefore, in the absence of diffuse scattering which should have indicated a local enlargement of the basic unit cell, we tried, in the same way as previous authors [8], to allow for ordering by a symmetry lowering within the non-centrosymmetric space group  $Bb$ . In this space group the refinements converged spontaneously to an ordering of the three  $\text{Na}^+$  ions on three different sites, the other possible sites being found to have essentially zero occupation 0.01(1). This was accompanied by a significant lowering of the  $R$  factor to a final value of 4.92%.

In the final stage further refinements based on third and fourth rank tensors, according to the Hermite polynomial expansion introduced by Johnson [19], for Na sites led to a significant improvement in the  $R$  factor, 4.51%, with important anharmonic corrections, especially for  $\text{Na}(1)'$  and  $\text{Na}(3)'$ .

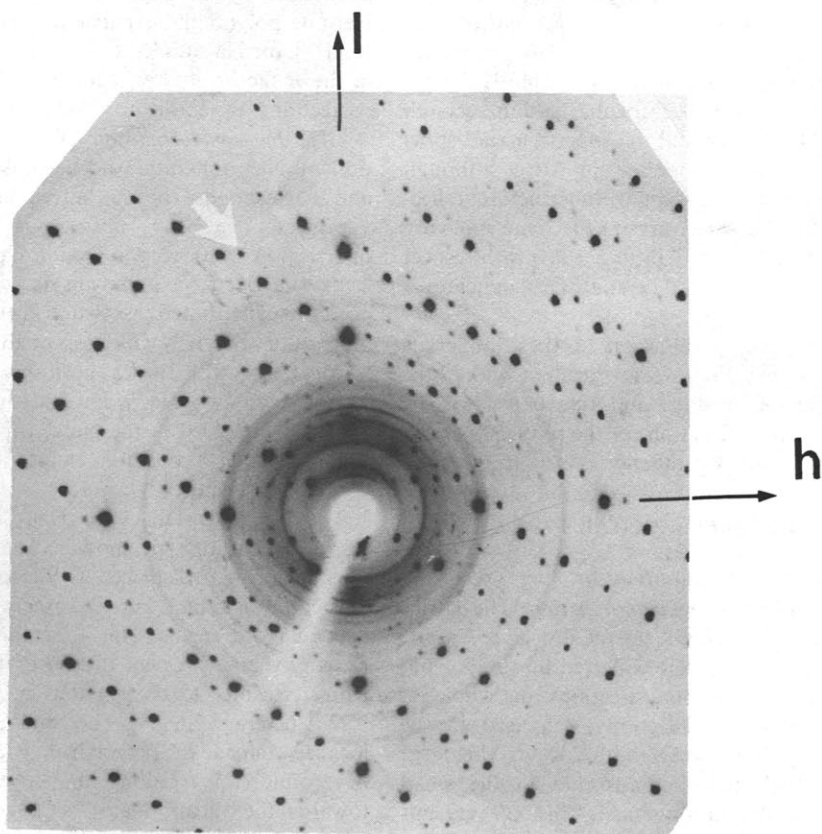
3.1.2. *Ion-ion correlations.* The schematic distribution of  $\text{Na}^+$  ions and vacancies is given Fig. 2(a) and corresponds to an "alternating packing" of vacancies. The  $\text{Na}(1)$  position is localized at the intersection of three conduction channels, and this leads to a given  $\text{Na}(1)$  having six neighboring  $\text{Na}(2)$  positions distributed as two triplets at  $z \pm \approx 1/12$  and rotated by  $\pi/3$  with respect to one another.

All the  $\text{Na}(2)$  triplet positions are equivalent, having each two  $\text{Na}^+$  ions and one vacancy. The vacancies involved in the  $\text{Na}(2)$  triplets surrounding the same  $\text{Na}(1)$  position cannot be in the same conduction channel.

The relevant distances are given Table 3 and in this low temperature type modification the conducting ions are strongly displaced with respect to their ideal Nasicon positions (Fig. 3) except for  $\text{Na}(2)'$ . In particular the regular  $\text{Na}(1)'$  octahedron appears to be empty and strongly distorted; the six distances from its center to oxygen ions being from 2.56 to 2.73 Å (average 2.68 Å). The  $\text{Na}(1)'$  ion of Table 2 is localized outside the octahedron, with a displacement of around 1.5 Å along the conduction channel, towards the vacant  $\text{Na}(3)'$  site, going through an octahedron face. This results in this  $\text{Na}(1)'$  site having a five-fold coordination; three  $\text{Na}(1)'$ -oxygen bonds are exchanged with the  $\text{O}^{2-}$  of the octahedron face



1 a



1 b

Fig. 1(a-b)

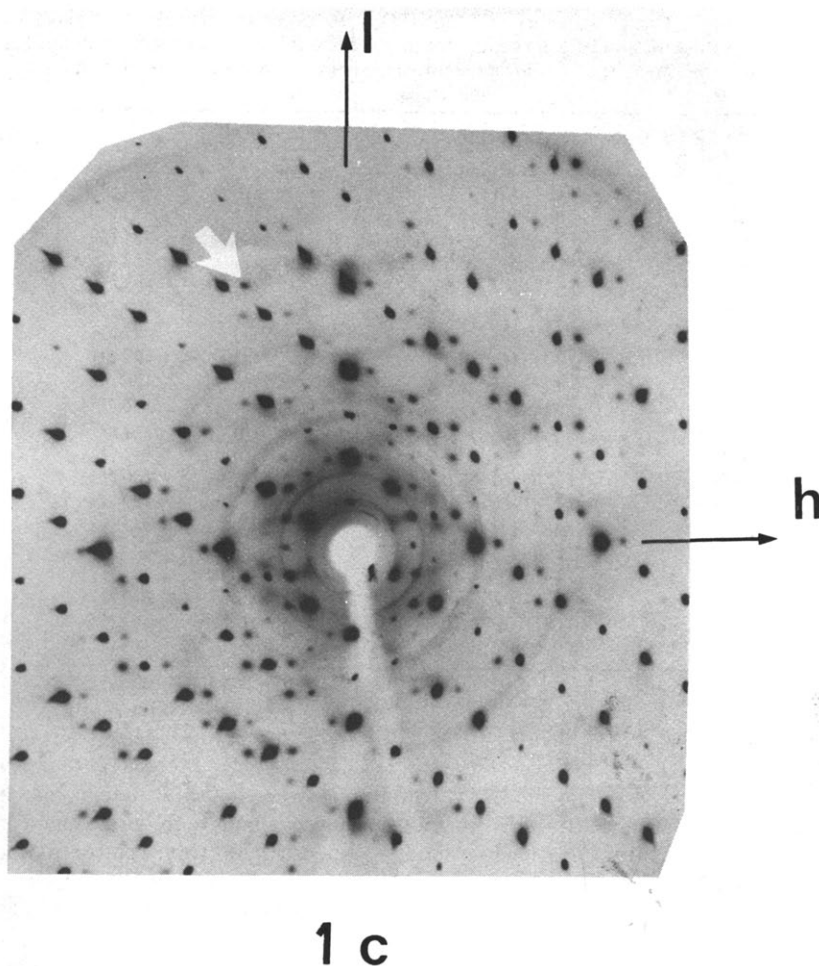


Fig. 1. Precession photographs of the  $h0l$  layer of the rhombohedral Nasicon sublattice (MoK $\alpha$ ). (1a) "Fusion" crystal. This layer corresponds to the  $h$ ,  $(-h + l)$ ,  $h$  monoclinic indices with a rotation axis which is not the unique monoclinic axis. The existence of rather strong forbidden reflections from the rhombohedral lattice (black arrow) suggests large amplitude displacements. (1b) "1470°C" crystal. This is strictly rhombohedral but with  $(2a, c)$  superstructure spots (white arrow) which correspond to long-range order. (1c) "Flux" crystal. This is also rhombohedral, with the same  $(2a, c)$  superstructure, but with diffuse spots (white arrow).

and two other bonds are exchanged with oxygen ions which normally depend on the Na(3)' coordination polyhedron.

The Na(3)' is also displaced along the conduction channel with respect to the ideal (rhombohedral) position, but with a smaller displacement amplitude  $\approx 0.5$  Å, and in the same direction as Na(1)', towards the octahedron (Fig. 3). This leads to a coordination of six instead of eight for a regular Na(2)-type site such as Na(2)'.

**3.1.3. The pseudoanti-Nasicon modification.** In Nasicon-type structure there is a constant source of confusion due to the pseudo-cubic lattice symmetry [7]. This leads for Nasicon analogs containing Sc, Cr or Fe, to two closely related kinds of indexing for the monoclinic unit cell, both with the same unique axis (Fig. 4). One of these orientations is referred to the rhombohedral lattice in the usual way, but the second presents a much more unusual relation. This second

orientation was that used in Ref. [8] by the authors to describe the pseudo "anti-Nasicon" modification. The results for the two possible orientations for our own crystal compared to the pseudo "anti-Nasicon" lattice constants of Ref. [8] are given in Table 4. The complete equality between the values of the last two lines clearly confirms that the pseudo "anti-Nasicon" is nothing but a simple rotation of the usual Nasicon lattice (which retains the  $B2/b$  or  $Bb$  symmetry as can be easily verified).

In our opinion this definitively establishes that monoclinic  $\text{Na}_3\text{Sc}_2(\text{PO}_4)_3$  exhibits only one modification with a slight deformation of the usual Nasicon lattice.

**3.1.4. Ionic distribution in Nasicon analogs.** In Table 5 are given the sodium occupancies on the different sites for the three  $\text{Na}_3\text{M}_2(\text{PO}_4)_3$  materials with  $\text{M} = \text{Sc}, \text{Cr}$  and  $\text{Fe}$ , in their monoclinic average lattice [16]. Table 5 explains why, although these

Table 2. Crystal structure of  $\text{Na}_3\text{Sc}_2(\text{PO}_4)_3$   $\alpha$ -type crystal obtained by fusion.  $\beta_{ij}$  values for atomic pairs deduced from the same  $B2/b$  position were constrained to refine together. No further improvement in the  $R$  factor was obtained for independent refinement

4a positions of $Bb$	$x$	$y$	$z$	$B_{\text{equi}} (\text{\AA}^2 \times 10^4)$
Na (1)'	0.1944 (5)	0.5577 (10)	0.1513 (6)	504 (35)
Na (2)'	-0.0021 (6)	0.2415 (12)	0.3907 (3)	353 (30)
Na (3)'	0.3286 (5)	0.3090 (10)	0.4251 (4)	331 (30)
P (1) $A$	0.3596 (4)	0.2622 (8)	0.1084 (2)	103 (5)
P (1) $B$	0.6444 (4)	0.7422 (8)	0.8916 (2)	103 (5)
P (2)	-0.0016 (4)	0.2506 (8)	0.0453 (1)	104 (10)
Sc	0.1019 (4)	0.0556 (8)	0.2462 (1)	82 (3)
Sc	0.9030 (4)	0.9529 (8)	0.7477 (1)	82 (3)
0 (1) $A$	0.1472 (6)	0.2198 (11)	0.4372 (6)	136 (13)
0 (1) $B$	0.8538 (6)	0.7828 (11)	0.5612 (6)	136 (15)
0 (2) $A$	0.4370 (6)	0.0863 (11)	0.4496 (6)	141 (15)
0 (2) $B$	0.5332 (6)	0.9166 (11)	0.5510 (6)	141 (15)
0 (3) $A$	0.2565 (6)	0.2083 (11)	0.1815 (6)	180 (15)
0 (3) $B$	0.7481 (6)	0.7899 (11)	0.8231 (6)	180 (15)
0 (4) $A$	0.3845 (7)	0.1241 (12)	0.1286 (7)	245 (18)
0 (4) $B$	0.6244 (7)	0.8863 (12)	0.8669 (7)	245 (18)
0 (5) $A$	0.4467 (6)	0.4370 (12)	0.1814 (6)	149 (17)
0 (5) $B$	0.5591 (6)	0.5676 (11)	0.8208 (6)	149 (17)
0 (6) $A$	0.0758 (6)	0.2418 (11)	0.1495 (6)	169 (15)
0 (6) $B$	0.9201 (6)	0.7626 (11)	0.8581 (7)	169 (15)

$a = 15.404$  (4)  $\text{\AA}$ ,  $b = 9.103$  (3)  $\text{\AA}$ ,  $c = 8.919$  (2)  $\text{\AA}$ ,  $\gamma = 123.53$  (2)°,  $R = 4.51\%$  for 2007 independent reflections.  $B_{\text{equi}}$  is defined by the expression  $B_{\text{equi}} (\text{\AA}^2) = \sum_{i,j} U_{ij}^* \mathbf{a}_i \mathbf{a}_j$ .

three materials have similar monoclinic low temperature distortions and chemical formula, they exhibit three different kinds of  $\text{Na}^+$ /vacancy ordering and consequently three distinct kinds of thermal behavior.

Table 3. Significant interionic distances ( $\text{\AA}$ ) in  $\alpha$ -type crystal, "fusion"

Na (1)'	0 (1) <i>B</i>	2.31	} octahedron face
	0 (3) <i>B</i>	2.36	
	0 (6) <i>A</i>	2.41	
	0 (2) <i>B</i>	2.47	} vacant Na (3)' polyhedron
	0 (5) <i>B</i>	2.62	
Na (3)'	0 (3) <i>A</i>	2.38	
	0 (2) <i>A</i>	2.40	
	0 (1) <i>A</i>	2.44	
	0 (3) <i>B</i>	2.52	
	0 (6) <i>B</i>	2.56	
	0 (5) <i>A</i>	2.65	
Na (2)'	0 (1) <i>A</i>	2.45	
	0 (6) <i>A</i>	2.46	
	0 (1) <i>B</i>	2.48	
	0 (5) <i>A</i>	2.51	
	0 (6) <i>B</i>	2.58	
	0 (4) <i>A</i>	2.58	
	0 (5) <i>B</i>	2.64	
	0 (4) <i>B</i>	2.72	
Tetrahedra		Average distances	
<P 1 <i>A</i> - 0>		1.53	
<P 1 <i>B</i> - 0>		1.53	
<P 2 - 0>		1.53	
Octahedra			
<Sc <i>A</i> - 0>		2.09	
<Sc <i>B</i> - 0>		2.09	

However, the scandium material exhibits the closest analogy to zirconium–Nasicon for which Wuensch [20], from neutron diffraction experiments on powders, established that, at room temperature, the Na(1) site is fully occupied and displaced, and the Na(2)' site is systematically more filled than the Na(3)' site. This analogy confirms the special role of  $\text{Na}_3\text{Sc}_2(\text{PO}_4)_3$  in Nasicon simulations.

### 3.2. The rhombohedral modifications

3.2.1. *Crystal structures.* Data were collected for both rhombohedral "1470°C" and "flux" crystals with  $\text{MoK}\alpha$  radiations up to  $2\theta = 65^\circ$ . After absorption corrections and averaging of equivalent reflections this led respectively to 668 and 667 independent reflections which were all used in the refinements, including the zero intensity reflections (6 and 9, respectively).

The calculations were carried out within the usual  $R\bar{3}c$  space group of Nasicon with simultaneous refinement of spatial coordinates, anisotropic temperature factors and occupancy factors of the two sodium sites. This resulted in rather low  $R$  factors of 2.84 and 2.93%, but with total Na occupancies which appreciably differed from three  $\text{Na}^+$  per unit formula, i.e. 2.84(3), with 0.70(1) Na(1) and 2.14(2) Na(2) for "flux" crystal, and 2.88(3), with 0.79(1) Na(1) and 2.09(2) Na(2) for "1470°C" crystal.

This is a problem we previously encountered with the first crystal we examined, which gave only 2.93(3)  $\text{Na}^+$  per unit formula [3]. Other authors [11, 13] have obtained even larger  $\text{Na}^+$  deficiencies as mentioned in the Introduction. This difficulty can be solved by

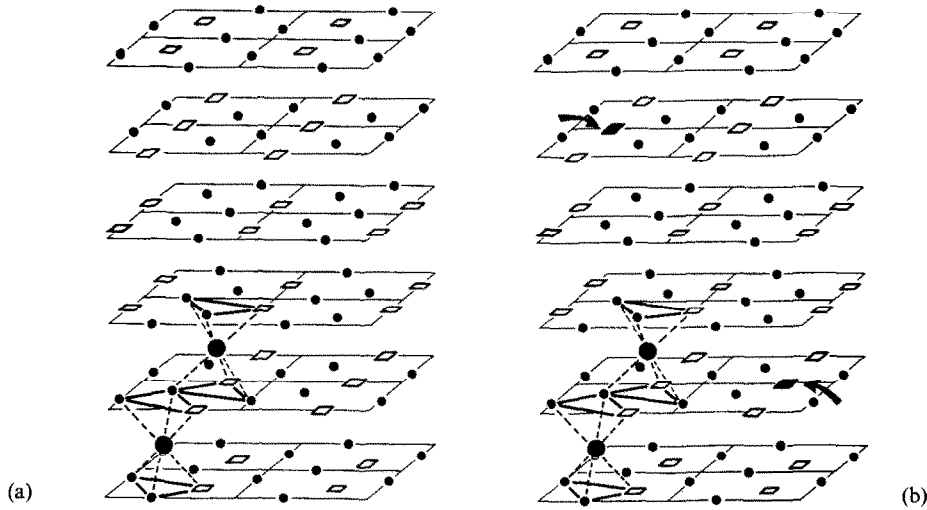


Fig. 2. Schematic distribution of vacancies in the rhombohedral Nasicon structure. Small circles correspond to occupied Na (2) positions, white squares to Na (2) vacant sites and large circles to Na (1) positions. Only two Na (1) are represented in order to make clear the definition of Na (2) triplets; they correspond to three Na (2) positions within the same basal plane, with conduction channels leading to the same Na (1) ion. (2a) Na<sup>+</sup>-vacancy distribution in the monoclinic  $\alpha$ -phase, "fusion" crystal. The ion shifts are not indicated. (2b) Na<sup>+</sup>-vacancy distribution in the  $(2a,c)$  superstructure of the  $\beta$ -phase, "1470°C" crystal. The black squares indicate the additional filled Na site compared to Fig. 2(a).

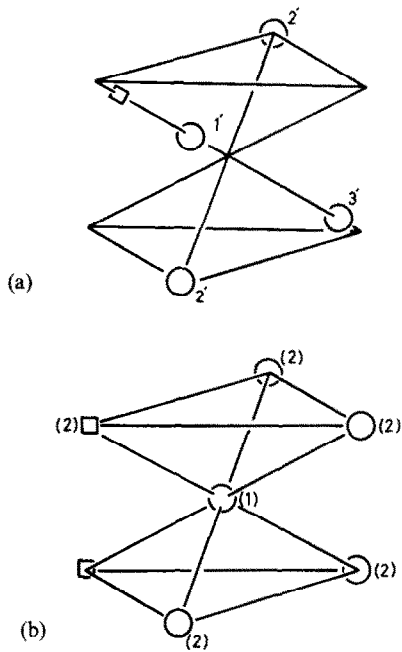


Fig. 3. Two Na (2) triplets related to the same Na (1). (3a) In the monoclinic  $\alpha$ -phase with strong displacements of Na<sup>+</sup> ions, 1.5 Å for Na (1) and 0.5 Å for Na (3). (3b) In the average  $\beta$  and  $\gamma$  lattices.

introducing anharmonic corrections to the Debye-Waller factors. In superionic conductors the shapes of the potential wells deviate considerably from a regular parabolic shape. In order to reduce the number of additional variables parameters, contracted tensors or scalars were used as far as possible.

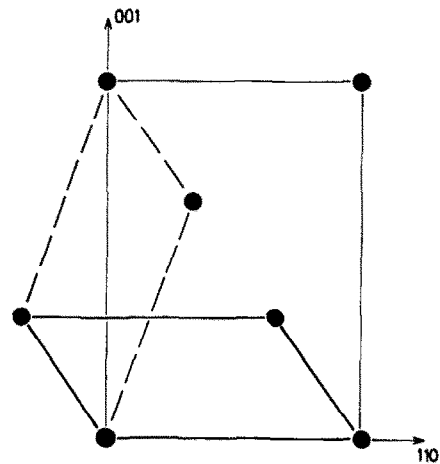


Fig. 4. Construction of the monoclinic cell starting from the rhombohedral (trigonal) lattice. Full lines indicate the regular cell used in this work, dotted lines the pseudo "anti-Nasicon" cell of Ref. [8]. The 2-fold axis ( $a_{\text{reg}}$ ) is normal to the plane.

Table 4. Monoclinic lattice constants of the Na<sub>3</sub>Sc<sub>2</sub>(PO<sub>4</sub>)<sub>3</sub> "fusion" crystal with the two possible unit cells compared to the pseudo "anti-Nasicon" results of Ref. [8]

		$a$ (Å)	$b$ (Å)	$c$ (Å)	$\gamma$ (°)
Our crystal	first unit cell	15.404 (4)	9.103 (3)	8.919 (2)	123°53 (2)
	second unit cell	16.093 (5)	9.103 (3)	8.919 (2)	127°07 (3)
	Ref. [8]	16.10 (1)	9.109 (4)	8.928 (4)	127°15 (4)

Table 5. Sodium occupancies for the different monoclinic sites in Nasicon-analogs  $\text{Na}_3\text{M}_2(\text{PO}_4)_3$ 

Maximum Na occupancy	Na (1) 1	Na (2) 1	Na (3) 2
Sc	1 Na <sup>+</sup>	1 Na <sup>+</sup>	1 Na <sup>+</sup> + 1 □
Cr	5Na <sup>+</sup> /6 + 1□/6	5 Na <sup>+</sup> /6 + 1□/6	4 Na <sup>+</sup> /3 + 2□/3
Fe	1 Na <sup>+</sup>	2 Na <sup>+</sup> /3 + 1□/3	4 Na <sup>+</sup> /3 + 2□/3

Full third and fourth rank tensors were applied only to the two Na sites.

Table 6 gives, as an example, the results of the "flux" crystal at each step in the refinement process involving the introduction of a new set of variable parameters. This shows that all the *R*-factor improvements are highly significant. As expected, the final Na composition corresponds closely to the ideal  $\text{Na}_3\text{Sc}_2(\text{PO}_4)_3$  formula (Table 7). We emphasize the fact that this result is obtained with simultaneous refinement of all variable parameter including occupancy factors. The two crystals may therefore be considered to a high degree of precision as corresponding to the ideal Nasicon formula.

**3.2.2. The (2a,c) superstructure.** In the "1470°C" and "flux" crystals the results of the refinements yield the statistical occupancy of both Na sites within the rhombohedral average lattice. The existence of the (2a,c) superstructure observed in both crystals [Fig. 1(b) and (c)] is clearly related to local correlations between conducting ions. With the "1470°C" crystal the superstructure spots are intense enough for data to be collected on a four-circle diffractometer at least around the origin of reciprocal space. Data were collected for reflections with indices  $0 \leq h, k \leq 10$ ,  $-20 \leq l \leq 20$  and  $2\theta \leq 40^\circ$  (MoK $\alpha$ ). This leads to 2414 superstructure reflections among which only 954 could be considered as observed ( $1 \geq \sigma$ ).

Given the large unit cell it was not possible to perform a complete calculation, since this would have led to an excessive number of variable parameters. Thus only the contribution of Na and vacancies to pure superstructure reflections ( $h$  and/or  $k \neq 2n$ ) was examined.

The apparent space group is  $P\bar{3}1c$ , in agreement with previous observations [13]. However refinements within this hypothesis gave a distribution of vacancies with very little order and high *R* factors ( $R > 45\%$ ). This indicates that the local correlations are not trigonal.

The simplest model is therefore a tri-twinned monoclinic (microtwin) model which retains the trigonal symmetry. In the centrosymmetric model (*B2/b*) the rhombohedral Na(1) and Na(2) positions are split respectively into six and 19 independent positions. The structural solution is given schematically, Fig. 2(b), and appears to be a slight modification of the vacancy ordering found for the monoclinic modification (cf. previous section). The final *R* factor of 15.3% for the 954 independent reflections can be considered as satisfactory in this

case. Indeed, since only Na<sup>+</sup> ions were considered, the relaxations of the other ionic positions are neglected and this makes it impossible to allow for the important displacive factors responsible especially for the progressive increase of intensities observed with increasing reciprocal distances. Moreover the thermal motions of the Na<sup>+</sup> sites were kept isotropic, a rather bad approximation.

As a consequence of this crude model, only the Na(2) vacancy ordering could be obtained. The localization of vacancies on the Na(1) sites could not be determined because the correlation terms in the refinement were much too high. Furthermore this determination should have required a further lowering of symmetry from *B2/b* to *Bb*, with 48 independent Na positions. This could not reasonably be carried out with the available data.

For the Na(2) type sites [Fig. 2(b)] on four Na(2) planes out of six the vacancies are distributed according to a two-dimensional (*a*\**a*) sublattice, but in a way impossible to account for within trigonal symmetry. The Na/vacancy distribution is unchanged in these planes with respect to the monoclinic modification with two Na<sup>+</sup> and one vacancy per Na(2) triplet. On the two other Na(2) planes there are only three vacancies for four Na(2) triplets. It is these planes which give the major contribution to the superstructure intensities.

A striking feature after the partial filling of the Na(2) sites is the ionic relaxation. This is spectacular for the Na(1) planes localized between unperturbed Na(2) planes, in which the Na<sup>+</sup> ions are found strictly on their ideal positions (Na 1-1 and 1-2, Table 9).

Finally the theoretical ionic distribution for this phase is 0.917 (or 11/12) Na(1) and 2.083 (or 25/12) Na(2). This explains why the superstructure has long range correlations in the "1470°C" crystal for which the composition closely corresponds to this formula. In contrast, in the "flux" crystal, more than twice too many Na(2) triplets are filled with respect to the ideal distribution, in agreement with the limited coherence length observed for this crystal for the superstructure [Fig. 1(c)].

### 3.3. Comparison between the three modifications

The results of the crystal structure determinations strongly confirm the initial hypothesis that each one of the three crystals corresponds to a given physical state. For the  $\alpha$ -type, "fusion", there is an average monoclinic lattice with complete ordering of Na<sup>+</sup>



Table 6. Statistical test of significance [25] for the introduction of anharmonic parameters into the refinement of the structure of the "flux" crystal

	Number of variable parameters	Minimum level of significance ( $\alpha = 0.005$ )	$R_1/R_2$	Na (1) occupancy	Na (2) occupancy	Total Na occupancy
Harmonic approximation ( $R = 2.84\%$ )	37	1.000	1.000	0.70 (1)	2.14 (2)	2.84 (3)
Contracted covariant tensors for oxygen	55	1.034	1.109	0.70 (1)	2.17 (2)	2.87 (3)
Full contravariant tensors for Na (2)	68	1.027	1.036	0.70 (1)	2.18 (3)	2.88 (4)
Full contravariant tensors for Na (1)	73	1.015	1.047	0.79 (2)	2.18 (2)	2.97 (4)
Contracted covariant $\gamma$ and scalar $\delta$ tensors for P and Sc	77	1.012	1.008	0.79 (2)	2.19 (2)	2.98 (4)

Anharmonic expansion of temperature factors was performed according to the Gram-Charlier type expansion introduced by Johnson [19].

Table 7(a). Coordinates and thermal parameters ( $\text{\AA}^2 \times 10^4$ ) of  $\text{Na}_3\text{Sc}_2(\text{PO}_4)_3$  "1470°C" crystal

	Max occup.		x	y	z	$U_{11}$	$U_{22}$	$U_{33}$	$U_{12}$	$U_{13}$	$U_{23}$
Sc	2	2	0	0	0.14861 (2)	95 (1)	$U_{11}$	92 (2)	$U_{11}/2$	0	0
P	3	3	0.29506 (5)	0	1/4	83 (2)	98 (2)	195 (3)	$U_{22}/2$	$U_{23}/2$	52 (2)
0 (1)	6	6	0.18607 (17)	-0.02295 (18)	0.19457 (7)	244 (6)	328 (7)	453 (8)	145 (5)	-177 (6)	75 (6)
0 (2)	6	6	0.19204 (14)	0.17278 (14)	0.08839 (5)	111 (5)	142 (5)	242 (5)	13 (4)	61 (4)	49 (4)
Na (1)	1	0.92 (2)	0	0	0	2306 (41)	$U_{11}$	244 (18)	$U_{11}/2$	0	0
Na (2)	3	2.08 (2)	0.63701 (17)	0	1/4	192 (6)	183 (8)	983 (15)	$U_{22}/2$	$U_{23}/2$	254 (9)

 $a = 8.927$  (1)  $\text{\AA}$ ,  $c = 22.276$  (3)  $\text{\AA}$ ,  $R = 2.35\%$  for 667 independent reflections.Table 7(b). Coordinates and thermal parameters ( $\text{\AA}^2 \times 10^4$ ) of  $\text{Na}_3\text{Sc}_2(\text{PO}_4)_3$  "flux" crystal

	Max occup.		x	y	z	$U_{11}$	$U_{22}$	$U_{33}$	$U_{12}$	$U_{13}$	$U_{23}$
Sc	2	2	0	0	0.14901 (2)	100 (2)	$U_{11}$	117 (2)	$U_{11}/2$	0	0
P	3	3	0.29612 (6)	0	1/4	95 (2)	104 (2)	198 (2)	$U_{22}/2$	$U_{23}/2$	54 (2)
0 (1)	6	6	0.18753 (19)	-0.02190 (20)	0.19442 (8)	290 (7)	386 (8)	502 (9)	163 (6)	-206 (7)	75 (7)
0 (2)	6	6	0.19163 (15)	0.17296 (15)	0.08809 (6)	131 (5)	145 (5)	280 (5)	9 (5)	54 (5)	54 (4)
Na (1)	1	0.79 (2)	0	0	0	1560 (40)	$U_{11}$	227 (40)	$U_{11}/2$	0	0
Na (2)	3	2.19 (2)	0.63778 (22)	0	1/4	212 (9)	195 (15)	991 (30)	$U_{22}/2$	$U_{23}/2$	220 (12)

 $a = 8.950$  (2)  $\text{\AA}$ ,  $c = 22.230$  (4)  $\text{\AA}$ ,  $R = 2.34\%$  for 668 independent reflections.

Table 8. Some significant interionic distances (Å) in "1470°C" crystal ( $\beta$ -type) and in "flux" crystal ( $\gamma$ -type)

Distances	Number of bonds	Distances crystal (1470°C) $\beta$	(Å) crystal (flux) $\gamma$
$\langle \text{P} - \text{O} \rangle$	4	1.525	1.525
$\langle \text{Sc} - \text{O} \rangle$	6	2.082	2.086
Na (1) - O (2)	6	2.559	2.550
Na (2) - O (2)	2	2.464	2.469
0 (2)	2	2.499	2.508
0 (1)	2	2.703	2.694
0 (1)	2	2.908	2.913
$\langle \text{Na} (2) - \text{O} \rangle$	8	2.644	2.646

and vacancies. The Na(1) site is fully occupied and strongly displaced. In this  $\alpha$ -type, all Na(2) triplets are constituted with two  $\text{Na}^+$  ions and one vacancy.

For the  $\beta$ -type, "1470°C", there is an average rhombohedral lattice with long range ordering of  $\text{Na}^+$  and vacancies, at least for Na(2) ions. The Na(1) sites are partially vacant (8%) and the ionic displacements are appreciably relaxed. In this  $\beta$ -type 1/12 of the Na(2) triplets are now occupied by three  $\text{Na}^+$  ions. For the  $\gamma$ -type, "flux", there is again an average rhombohedral lattice, but with only short-range order of  $\text{Na}^+$  and vacancies. The Na(1) site is appreciably vacant ( $\approx 20\%$ ). In this  $\gamma$ -type at least

Table 9. Na position of the (2a,c) superstructure

	x	y	z	$\Delta$ (Å)
8 Na 1-1	0.000 (3)	0.000 (3)	0.250 (5)	0.00
8 Na 1-2	0.250 (3)	0.000 (3)	0.000 (5)	0.00
8 Na 1-3	0.172 (2)	0.175 (2)	0.308 (3)	1.05
8 Na 1-4	0.174 (2)	0.175 (2)	0.808 (3)	1.05
8 Na 1-5	0.423 (2)	0.177 (2)	0.061 (4)	1.12
8 Na 1-6	0.923 (2)	0.173 (2)	0.061 (4)	1.12
8 Na 2-1	-0.001 (1)	0.070 (1)	0.410 (2)	0.44
8 □	0.174	0.083	0.409	
8 Na 2-3	0.073 (1)	0.089 (2)	0.695 (3)	0.46
8 Na 2-4	0.496 (1)	0.074 (1)	0.407 (2)	0.27
8 □	0.674	0.083	0.409	
8 Na 2-6	0.574 (1)	0.088 (2)	0.696 (2)	0.44
8 Na 2-7	0.251 (1)	0.077 (2)	0.158 (2)	0.35
8 □	0.424	0.083	0.159	
8 Na 2-9	0.323 (2)	0.091 (2)	0.452 (3)	0.57
8 Na 2-10	0.747 (2)	0.080 (2)	0.452 (3)	0.18
8 □	0.924	0.083	0.159	
8 Na 2-12	0.822 (2)	0.093 (2)	0.447 (3)	0.57
8 Na 2-13	0.165 (1)	0.251 (1)	0.089 (1)	0.18
8 Na 2-14	0.336 (1)	0.247 (1)	0.085 (1)	0.17
8 Na 2-15	0.413 (1)	0.262 (1)	0.339 (1)	0.24
8 Na 2-16	0.082 (1)	0.245 (1)	0.339 (1)	0.22
8 □	0.250	0.250	0.319	
4 Na 2-18	0.000	0.250	0.084 (1)	0.27
4 □	0.000	0.250	0.569	

The space group is  $B2/b$  and the description corresponds to one of the three samples of the microtwin with  $a_{\text{mono}} = a_{\text{trig}} + 2b_{\text{trig}}$ ,  $b_{\text{mono}} = c_{\text{trig}}$ ,  $c_{\text{mono}} = a_{\text{trig}}$ . Position Na 2-18 corresponds to the position initially vacant in the  $\alpha$ -form which is now filled.  $\Delta$  is the shift with respect to the ideal (rhombohedral) position (in Å).

more than 1/6 of Na(2) triplets are occupied by three sodium ions.

## 4. DISCUSSION

### 4.1. Composition

The three crystal structures found clearly indicate that the formula within the limit of standard deviations is  $\text{Na}_3\text{Sc}_2(\text{PO}_4)_3$  for the three materials examined, and that there is no evidence for a "non-stoichiometry" mechanism. Indeed no deviation from full occupancies was found for the scandium and phosphorus sites, the sum of the sodium occupancies spontaneously converged to 3.00, and the M-oxygen distances do not indicate anything unusual for any of the materials.

In contrast, in Zr-Nasicon materials, a "non-stoichiometry" mechanism exists [2], corresponding to an exchange of  $\text{Zr}^{4+}$  with  $\text{Na}^+$  within the octahedra. This leads, for charge compensation, to an excess of  $\text{Na}^+$  in the conduction channels (three additional  $\text{Na}^+$  ions per  $\text{Zr}^{4+}$  replaced). However in  $\text{Na}_3\text{Sc}_2(\text{PO}_4)_3$  an excess  $\text{Na}^+$  ions was not found in any crystal. On the contrary  $\text{Na}_{3.00}$  appears to be the upper limit, reached only when special care is taken during the refinement process. This leads us to suggest that the deficiency of  $\text{Na}^+$  encountered by various authors (see the Introduction) is due to refinement procedures using largely inadequate shapes for the potential wells of the conducting ions.

It is therefore concluded that the differences between the three crystals cannot be attributed to differences in compositions.

### 4.2. Raman spectra

Raman spectra were recorded with a Spectra-Physics argon ion laser using the 488.0 and 514.5 nm lines for excitation. The spectra corresponding to the three types of crystals exhibit some marked differences (Fig. 5). In the monoclinic  $\alpha$ -phase the band, in the range 900–1200  $\text{cm}^{-1}$ , resulting from the stretching modes of  $\text{PO}_4$  tetrahedra ( $\nu_1, \nu_3$ ) is split

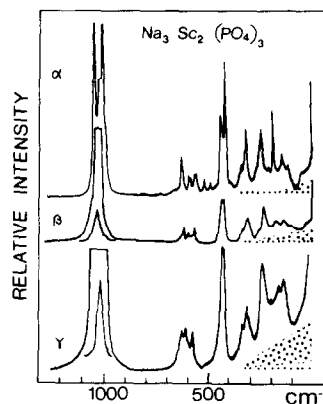


Fig. 5. Raman spectra at room temperature for the three different crystals of  $\text{Na}_3\text{Sc}_2(\text{PO}_4)_3$ .

into several modes in agreement with the monoclinic symmetry, exactly as observed for  $\text{Na}_3\text{Sc}_2(\text{PO}_4)_3$  powders [21]. However two additional features are present: (i) external tetrahedra modes (the  $250\text{ cm}^{-1}$  mode assigned to motion involving mainly tetrahedra libration), are broader than Sc modes such as the translational mode at  $190\text{ cm}^{-1}$  and (ii) a broad low frequency mode ( $\approx 40\text{ cm}^{-1}$ ) is observed corresponding to a librational mode of tetrahedra.

This shows that, in spite of the existence of long-range order associated with a low symmetry, an orientational disorder is present in these crystals.

In  $\beta$ -type crystals, the  $\nu_1$ - $\nu_3$  band consists only of a broad asymmetric peak ( $\Delta\nu_{1,2} \approx 40\text{ cm}^{-1}$ ), whereas the  $\nu_2$  and  $\nu_4$  modes remain split. This is consistent with the structural model (cf. the  $(2a,c)$  superstructure); local monoclinic symmetry with a lower distortion than in the  $\alpha$ -type crystals. In these spectra, in the low frequency region, a Rayleigh wing is observed superposed on the  $40\text{ cm}^{-1}$  mode.

Finally, in  $\gamma$ -type crystals, the  $\nu_1$ - $\nu_3$   $\text{PO}_4$  stretching modes are nearly symmetric and result in a very broad band ( $\Delta\nu_{1,2} \approx 50\text{ cm}^{-1}$ ), which indicates a high degree of disorder as found in "tetrahedral glasses" [22, 23]. In these materials the local environment exhibits a higher symmetry; however, there is some distortion as indicated by the splitting of the  $\nu_4$  modes. Furthermore the low frequency wing is now especially intense. This spectrum is quite equivalent to that observed for strongly disordered systems such as liquids, molten salts or glasses [24].

To sum up, main conclusion of this investigation is to show clearly the existence, in the three crystal-types, of a disorder of the  $\text{PO}_4$  tetrahedra, very noticeable in the rhombohedral  $\beta$ -phase and especially in the  $\gamma$ -phase, but already present to some extent in the most ordered  $\alpha$ -phase. In this domain, vibrational spectra provide very useful information concerning the nature of the disorder.

The existence of such a disorder has to be related to one of the essential characteristics of Nasicon-type materials, namely their tendency to form glasses easily. This is in agreement with a description in terms of a lattice of  $\text{PO}_4$  tetrahedra in which scandium and sodium ions occupy only vacant cavities between tetrahedra but do not contribute to the structural modifications. As might be expected, the consequence of loss of long-range correlations in Nasicon glasses produces effects quite similar to those observed for the  $\beta$  and  $\gamma$  phases of  $\text{Na}_3\text{Sc}_2(\text{PO}_4)_3$ , i.e. broadening of tetrahedra modes, presence of low-frequency background, etc.

#### 4.3. The disorder of tetrahedra

This disorder of tetrahedra indicated by Raman spectroscopy can also be verified by the structural results, which for the rhombohedral  $\beta$  and  $\gamma$  phases indicate an anomalously high temperature factor in the  $c_{\text{trig}}$  direction for phosphorus atoms;  $U_{33}$  is about twice the other principal components; these on the

contrary have normal values and are in the same range as those for scandium, which can be considered as a reference.

In addition there are exceptionally high vibration amplitudes for the anions, again in the  $c_{\text{trig}}$  direction, especially for oxygen atom O(1). This suggests the existence of rotational terms for the  $\text{PO}_4$  tetrahedron around the two-fold axis directed along the  $a$  trigonal lattice vector associated with a stretching of the O(1)-P-O(1) sequence along  $c_{\text{trig}}$ .

For the monoclinic  $\alpha$ -phase, as expected from the Raman results, these effects are strongly reduced. The different phosphorus atoms exhibit along the pseudo  $c_{\text{trig}}$  axis vibration amplitudes which are less than  $0.015\text{ \AA}^2$  and the corresponding terms of the oxygen atoms are on average only one-half of the values observed for the rhombohedral phases.

These structural results are in good agreement with the Raman results and confirm the existence of a significant disorder of the  $\text{PO}_4$  tetrahedra. This is also consistent with the lattice symmetry, and the results for the ion-ion correlations. Indeed, the static orientational disorder presents some analogy with the dynamical disorder introduced by heating and produces similar effects. (i) Relaxation of the monoclinic distortion with the occurrence of rhombohedral  $R\bar{3}C$  symmetry, as observed for the  $\beta$  and  $\gamma$  crystals. (ii) Reduction of the  $c$  lattice constant with respect to the ordered  $\alpha$ -phase;  $c_{\text{trig}} \approx 22.2$ – $22.3\text{ \AA}$  compared with  $22.7\text{ \AA}$  (projection) for the  $\alpha$ -phase (Table 1). (iii) Occurrence of a  $(2a,c)$  superstructure. (iv) Reduced occupancy of the Na(1) site due to a transfer of part of sodium ions into Na(2) sites. The occupation factors are 0.92 and 0.79, respectively for the disordered  $\beta$  and  $\gamma$  crystals at room temperature, whereas in the ordered  $\alpha$ -phase the Na(1) site was found completely filled.

These effects, produced by the disorder of tetrahedra, are also observed on heating the monoclinic  $\alpha$ -phase. At the first phase transition at  $323\text{ K}$ , the average rhombohedral symmetry is restored, accompanied by a decrease in the  $c_{\text{trig}}$  lattice constant from  $22.7\text{ \AA}$  to  $22.3\text{ \AA}$ . Moreover one observes also the appearance of a  $(2a,c)$  superstructure, quite similar to that described for the  $\beta$  and  $\gamma$  crystals, associated with a transfer of sodium ions from Na(1) into Na(2) sites.

This parallelism between both types of disorder then provides an explanation for the existence of the  $\beta$  and  $\gamma$  phases, which in some way appear to be stabilized high temperature modifications. As expected, the effects are greater for the  $\gamma$ -phase, in which a very advanced state of disorder is found.

#### 4.4. The temperature of preparation as a critical parameter

Under these conditions the critical parameter responsible for the occurrence of a particular structure clearly appears to be the temperature of preparation of crystals, a general characteristic of "glassy" mate-

rials. Indeed glasses are stable at low temperature, and annealing at high temperature induces their crystallization. It is easy to conclude that something similar happens with  $\text{Na}_3\text{Sc}_2(\text{PO}_4)_3$ . Crystals prepared at low temperature from flux, which is itself a "liquid" of  $\text{PO}_4$  ions (molten  $\text{Na}_3\text{PO}_4$ ), will logically present the highest degree of disorder, as is observed in the so-called  $\gamma$ -type crystals. A higher temperature of preparation,  $1470^\circ\text{C}$ , for  $\beta$ -type crystals and especially for  $\alpha$ -type crystals prepared just below the melting point, will provide sufficient energy to propagate strict long-range order correlations and hence decreased disorder, at least compared with the flux method.

Consequently the main contribution obtained from this investigation of the  $\text{Na}_3\text{Sc}_2(\text{PO}_4)_3$  materials is to show that residual static disorder of tetrahedra which occurs commonly with powders, can also be present to an appreciable extent with crystals.

This explains the apparently puzzling variety of published results on this material. Indeed, as the different authors used different methods, and especially different temperature, for their crystal growth, one can expect a distribution of results among the different possible types of crystals  $\alpha$ ,  $\beta$  or  $\gamma$ . Moreover these types are not strictly defined, and for example a complete continuity range may be predicted between the rhombohedral  $\beta$  and  $\gamma$  phases, with a more or less extended coherence length for the  $(2a,c)$  superstructure (Fig. 1). In contrast the  $\alpha$ - $\beta$  cross-over probably occurs in a rather limited temperature range.

Based on the conditions of preparation, lattice constants and site occupancies, it is possible to propose a classification of published results with respect to the three general modifications of  $\text{Na}_3\text{Sc}_2(\text{PO}_4)_3$ . To the most ordered  $\alpha$ -type "fusion", correspond the structural results of Efremov and Kalinin [8], within the restriction of the unusual lattice description retained by these authors, the results of Tchakev *et al.* [14], and the monoclinic crystals described by Susman *et al.* [12]. In addition, and in agreement with the results of these latter authors, this  $\alpha$ -type appears to be the most closely related to powders. To the  $\beta$ -type, " $1470^\circ\text{C}$ " crystal, correspond the crystal structure determination reported by Hong [11] (which is not really monoclinic as shown by Susman *et al.* [12] and confirmed by a partially vacant Na(1) site), and the results published by Tran Qui *et al.* [13], who pointed out the existence of condensed  $(2a,c)$  superstructure spots characteristic of the  $\beta$ -phase. Finally the crystals described in Refs [7] and [16] are related to the  $\gamma$ -type structure, which presents the highest degree of disorder.

In a subsequent paper, we will show that the differences between crystals due to more or less

extended disorder, are retained at high temperature, and also in particular that each crystal type exhibits a specific behavior which we will examine in relation to the conduction paths.

## REFERENCES

1. Goodenough J. B., Hong H. Y.-P. and Kafalas J. A., *Mat. Res. Bull.*, 203 (1976).
2. Boilot J. P., Collin G. and Comes R., *J. Solid State Chem.* **50**, 91 (1983).
3. Boilot J. P., Collin G. and Comes R., *Solid State Ionics* **9-10**, 829 (1983).
4. Boilot J. P., Colomban P. and Blanchard N., *Solid State Ionics* **9-10**, 639 (1983).
5. Susman S., Delbecq C. J., McMillan U. A. and Roche M. F., *Solid State Ionics* **9-10**, 667 (1983).
6. Delbecq C. J., Marshall S. A. and Susman S., *Solid State Ionics* **1**, 145 (1980).
7. Boilot J. P., Collin G. and Comes R., *Solid State Ionics* **5**, 307 (1981).
8. Efremov V. A. and Kalinin V. B., *Kristallografiya* **23**, 703 (1978).
9. Kalinin V. B., Lazoryak B. I. and Stefanovich S. Yu., *Kristallografiya* **28**, 264 (1983).
10. Lazoryak B. I., Kalinin V. B., Stefanovich S. Yu. and Efremov V. A., *Dokl. Akad. Nauk. SSSR* **250**, 861 (1980).
11. Hong H. Y. P., *Fast Ion Transport in Solids* (Edited by P. Vashishta, J. N. Mundy, G. K. Shenoy) p. 431. Elsevier, North Holland (1973).
12. Susman S., Delbecq C. J., Brun T. O. and Prince E., *Solid State Ionics* **9-10**, 839 (1983).
13. Tran Qui D., Capponi J. J., Gondrand M. and Joubert J. C., *Solid State Ionics* **5**, 305 (1981).
14. Tchakev V. V., Ponomarev V. I. and Atovmyan L. O., *Zh. Strukt. Khim.* **25**, 11 (1984).
15. Atovmyan L. O., Bukun N. G., Kovalenko V. I., Korosteleva A. I., Tchek V. V. and Ukshe E. A., *OOLP Nauk.*, SSSR **19**, 933 (1983).
16. de la Rochere M., D'Yvoire F., Collin G., Comes R. and Boilot J. P., *Solid State Ionics* **9-10**, 825 (1983).
17. d'Yvoire F., Pintard-Screpel M., Bretey and de La Rochere M., *Solid State Ionics* **9-10**, 851 (1983).
18. Collin G., Boilot J. P., de La Rochere M. and Comes R., *Conference Proceedings on High Temperature Solid Oxide Electrolytes*, Brookhaven (Edited by F. V. Salzano) p. 72 (1983).
19. Johnson C. K., *International Tables for X-ray Crystallography*, International Union of Crystallography, Kynoch Press, Birmingham, p. 313 (1974).
20. Wuensch B. V., Schioler L. J. and Prince E., *Conference Proceedings in High Temperature Solid Oxide Electrolytes*, Brookhaven (Edited by F. V. Salzano), p. 55 (1983).
21. Barj M., Perthuis H. and Colomban P., *Solid State Ionics* **9-10**, 846 (1983).
22. Teeters D. and Frech R., *Phys. Rev.* **B26**, 5897 (1982).
23. Barj M., Perthuis H. and Colomban P., *Solid State Ionics* **11**, 157 (1983).
24. Sharma S. K. and Simons B., *Ann. Mineral* **66**, 118 (1981).
25. Hamilton W. C., *International Tables for X-Ray Crystallography*, p. 287. International Union of Crystallography, Kynoch Press, Birmingham (1974).